

Scaling analysis of sediment equilibrium in aggregated colloidal suspensions

D. Senis and C. Allain

Laboratoire Fluides, Automatique et Systèmes Thermiques, Bâtiment 502, Campus Universitaire, 91405 Orsay Cedex, France

(Received 3 February 1997)

The equilibrium of aggregated colloidal suspensions under gravity is studied both theoretically and experimentally. Using a simplified model to describe the compaction of the gelled suspension, we show that the volume fraction of the particles needed to form a stable gel is not intrinsic to the physicochemical system but depends on the height of the sample, its aspect ratio, and the friction between the suspension and the cell wall. A scaling analysis is developed to predict the various regimes encountered and to calculate the variations of the equilibrium sediment height as a function of the volume fraction of the particles and the height, and width of the sample. Good agreement is found with systematic measurements performed on aqueous colloidal calcium carbonate suspensions. [S1063-651X(97)11106-0]

PACS number(s): 82.70.-y, 64.60.Fr, 62.20.Fe

Aggregation phenomena have been studied extensively in the past both experimentally and theoretically [1,2]. When the growth rate is controlled solely by the Brownian diffusion of aggregates, the growth kinetics, and the cluster fractal geometry are well understood. The diffusion-limited cluster aggregation model gives a good description of the experimental and numerical simulation results [2–5]. In the presence of a large difference between the density of the particle and that of the solvent, gravity acts as an external field and modifies the growth process [6–9]. In a recent work, we have shown that the coupling between settling and aggregation leads to distinct behaviors depending on the volume fraction of particles in the suspension Φ [8]. In the dilute regime $\Phi < \Phi^*$, deposition of individual clusters is observed. At the beginning of the phenomenon, the aggregate growth is controlled solely by Brownian diffusion. As their size becomes large enough, they settle separately and deposit onto the cell bottom, forming a sediment that compacts until equilibrium. In the semidilute regime $\Phi^* < \Phi < \Phi^{**}$, a collective behavior is observed. A close packing of aggregates filling the whole cell (i.e., a gel) forms very rapidly and collapses under its own weight. A sharp interface separates a clear supernatant from the suspension; this interface moves down until it reaches its equilibrium height. Finally, when $\Phi > \Phi^{**}$, the suspension forms a gel that does not collapse under gravity. A scaling analysis based on the comparison between the gel time and the time corresponding to the crossover from diffusive to settling movements allows one to predict Φ^* [8].

The main objective of this paper is to determine the volume fraction Φ^{**} . We develop a simple model describing gel compaction and equilibrium under gravity. The predictions are compared to measurements of the relative volume occupied by the sediment: $\Omega = H_s/H$, where H_s represents the sediment height at equilibrium. A broad range of experimental conditions has been investigated by varying the volume fraction of the suspension, the height H , and the diameter D of the sample. We find that different regimes can be distinguished following the volume fraction and the sample sizes. Using a scaling analysis, we interpret the variations observed for Ω and we show that the volume fraction Φ^{**} is

not only intrinsic to the physicochemical system, but depends on the sample height and width.

The experiments have been done with colloidal suspensions of calcium carbonate in water. The particles (Socal U1 supplied commercially by Solvay Co) are prepared by precipitation; their density is $\rho = 2.7 \text{ g/cm}^3$ and their radius 35 nm. Under our experimental conditions (free atmosphere, $[\text{Ca}^{2+}] \approx 10^{-4} \text{ mol/L}$, and pH ranging between 8.7 and 9.2), the charge borne by the particles is very small ($\psi_s < 10 \text{ mV}$) and the colloidal interaction is given by the van der Waals potential. The samples were carefully prepared to ensure a good dispersion of the particles [8]. The cells used for the settling experiments, made from Plexiglas, are cylindrical. The accuracy on the determination of the relative sediment height Ω is about $\Delta\Omega = \pm 0.05$ [10].

Figures 1–3 display the variations of the sediment relative volume Ω versus the volume fraction of the suspension, the height, and the diameter of the sample. Even for small values of Φ , large values of Ω are observed (see Fig. 1): For $\Phi = 0.05$, the sediment occupies almost half of the cell. This shows that sediments formed by aggregated colloidal suspen-

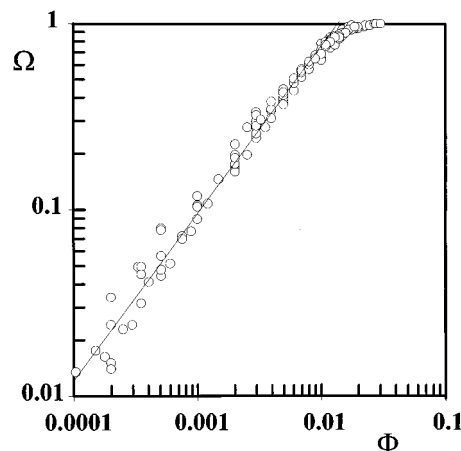


FIG. 1. A log-log plot of the relative sediment volume Ω versus the particle volume fraction Φ . The sample is $H = 70 \text{ mm}$ in height and its diameter is $D = 12 \text{ mm}$. The solid line corresponds to the scaling law given by Eq. (6) (domain II).

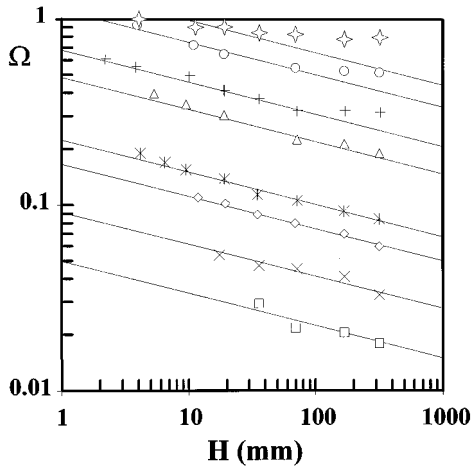


FIG. 2. A log-log plot of Ω versus H for different values of the particle volume fraction Φ : (\diamond), 0.01; \circ , 0.007; +, 0.004; Δ , 0.002; *, 0.001; \diamond , 0.0005; \times , 0.00035; \square , 0.0002. The diameter is $D = 12$ mm. The solid line corresponds to the scaling law given by Eq. (6) (domain II).

sions are very tenuous. Since $\Phi^* \cong 3 \times 10^{-3}$ [8], the studied samples belong to both the dilute and semidilute regimes ($\Phi < \Phi^*$ and $\Phi > \Phi^*$). In practice, no change in the variation of Ω is observed for $\Phi \cong \Phi^*$. On Fig. 2, a net decrease of Ω with H is observed: about a factor 2 for H varying from 2 to 320 mm. This reveals that sediments compact. Indeed, when a sediment is incompressible, Ω is independent of H . Here, as H becomes larger, the increase of the stress at a given height in the sample leads to a larger compaction: The local volume fraction φ increases. So the sediment is more concentrated and its relative volume is lower. Ω also decreases with the diameter D (see Fig. 3): For large values of D , Ω is constant, but Ω increases as D decreases. This effect comes from the existence of friction between the gel and the vertical cell side. This friction hindering gel compaction leads to a larger value of the sediment volume.

Let us now consider the equilibrium of a sediment layer under gravity. In a one-dimensional model, the force balance equation is expressed as

$$-\Delta\rho g\varphi = \frac{\partial\sigma}{\partial z} - \frac{4\mu\alpha}{D}\sigma. \quad (1)$$

The first term in Eq. (1) comes from the gravitational field: $\Delta\rho$ is the difference between the density of the particles and that of the solvent and g is the acceleration of gravity. σ is the stress at height z ; the z axis is oriented upward and $z=0$ corresponds to the bottom of the sample. The last term on the right-hand side of Eq. (1) comes from the friction between the gel and the vertical wall cell: The wall stress due to friction is assumed to be expressed as $\sigma_w = \mu\alpha\sigma$, where μ is the friction coefficient involved in the law of Amontons and α is a constant that relates σ to the radial stress. Note that, although this description of friction is exact for usual solids, for a compacted gel, $\mu\alpha$ may depend on σ , on the local value of volume fraction, or on the history of compaction. In the following, we do not consider such effects and we assume $\mu\alpha$ to be constant. Finally, to calcu-

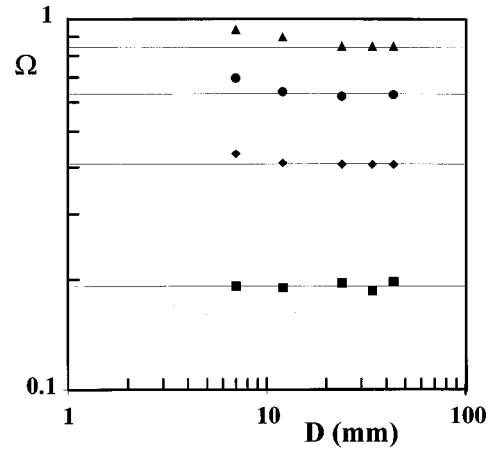


FIG. 3. A log-log plot of Ω versus D for different values of the particle volume fraction Φ : \blacktriangle , 0.013; \bullet , 0.01; \blacklozenge , 0.005; \blacksquare , 0.002. The height is $H = 70$ mm. The solid line corresponds to the scaling law given by Eq. (6) (domain II).

late the sediment equilibrium, we have to take into account the mechanical properties of the gel. We use here a simplified description based on the following assumptions. First, elastic deformations are assumed to be negligible and the gel to irreversibly compact when σ exceeds the yield stress value σ^Y . So when $\sigma \leq \sigma^Y$ the gel resists without any deformation and when $\sigma > \sigma^Y$ the gel consolidates, i.e., its local volume fraction φ increases until $\sigma^Y(\varphi)$ exactly counterbalances the stress σ . Second, σ^Y is assumed to depend solely on φ and to follow a power-law dependence

$$\sigma^Y(\varphi) = \sigma_0\varphi^\kappa, \quad (2)$$

where σ_0 represents the prefactor and κ the exponent, which is known to be very large. Rheological investigations and measurements done under either centrifugal acceleration or pressure filtration have shown that κ is of the order of 4–5 [11–13].

Equations (1) and (2) involve two different length scales: a vertical one and a horizontal one. Let us first consider the vertical scale length Λ , which is the only length involved in the absence of friction between the gel and the vertical cell side ($\mu\alpha \rightarrow 0$ or $D \rightarrow \infty$). The maximum of the compressive stress (which is observed in $z=0$) is then equal to $\Delta\rho g H \Phi$. Comparing this value to the yield stress $\sigma^Y(\Phi)$ leads to the introduction of

$$\Lambda = \frac{\sigma_0\Phi^{\kappa-1}}{\Delta\rho g} = \Lambda_0\Phi^{\kappa-1}. \quad (3)$$

Let us now consider the other limit where friction is the leading effect. The stress is then independent of z and equal to $\sigma = (1/4\mu\alpha)D\Delta\rho g\Phi$. Comparing this value to the yield stress leads to the introduction of the horizontal length scale Γ ,

$$\Gamma = \frac{4\mu\alpha\sigma_0\Phi^{\kappa-1}}{\Delta\rho g} = \Gamma_0\Phi^{\kappa-1} = 4\mu\alpha\Lambda. \quad (4)$$

Depending on the values of Λ and Γ compared to the height H and diameter D of the sample, different cases can be distinguished (see Fig. 4). In the limit of small heights,

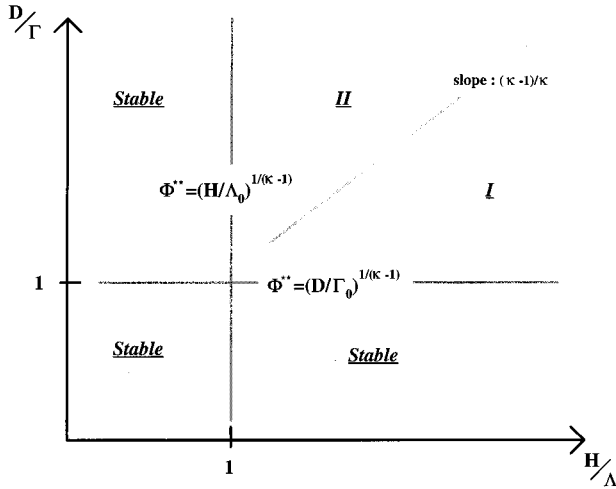


FIG. 4. Schematic diagram showing the different regimes (log representation).

i.e., $H/\Lambda \ll 1$, the maximum stress in the gel does not exceed $\sigma^Y(\Phi)$ and the gel resists whatever D/Γ is. The volume fraction that corresponds to $H=\Lambda$ [i.e., $\sigma_{\max}=\sigma^Y(\Phi)$] is Φ^{**} . When the contribution of friction is negligible ($D/\Gamma \gg 1$), $H=\Lambda$ leads to $\Phi^{**}=(H/\Lambda_0)^{1/(\kappa-1)}$. In the limit of small diameters $D/\Gamma \ll 1$, the gel is stable under gravity whatever H/Λ is. The volume fraction Φ^{**} can be calculated as previously by setting $D=\Gamma$. If the contribution of friction is dominant then $\Phi^{**}=(D/\Gamma_0)^{1/(\kappa-1)}=(D/4\mu\alpha\Lambda_0)^{1/(\kappa-1)}$.

When the suspension separates by compacting ($H/\Lambda \gg 1$ and $D/\Gamma \gg 1$), the relative volume of the sediment at equilibrium can be calculated from Eqs. (1) and (2). Two cases can be considered, depending on the relative importance of the two terms on the right-hand side of Eq. (1). In the limit where friction is dominant, which corresponds to $\Gamma/D \gg \Lambda/H_S$, i.e., $D/H \ll 4\mu\alpha\Omega$ (domain I in Fig. 4), φ and Ω can be easily derived. φ is independent of z . $\varphi=(D/\Gamma_0)^{1/(\kappa-1)}$ and Ω is expressed as

$$\Omega = \left(\frac{D}{\Gamma}\right)^{-1/(\kappa-1)} = \left(\frac{D}{\Gamma_0}\right)^{-1/(\kappa-1)} \Phi. \quad (5)$$

In the limit where friction is negligible ($D/H \gg 4\mu\alpha\Omega$, domain II in Fig. 4), the profile of local volume fraction φ can also be calculated analytically. If we assume that compaction occurs at every height

$$\varphi = \{(H\Phi/\Lambda_0)^{(\kappa-1)/\kappa} - [(\kappa-1)/\kappa](z/\Lambda_0)\}^{1/(\kappa-1)}.$$

Then, setting the conservation of the total particle volume, Ω is found to behave as

$$\Omega = \frac{\kappa}{\kappa-1} \left(\frac{H}{\Lambda}\right)^{-1/\kappa} = \frac{\kappa}{\kappa-1} \left(\frac{H}{\Lambda_0}\right)^{-1/\kappa} \Phi^{(\kappa-1)/\kappa}. \quad (6)$$

Now, if we take into account the layer near the top of the sediment where σ does not exceed $\sigma^Y(\Phi)$ (i.e., where compaction does not occur), Ω is multiplied by a correcting factor $1-(1/\kappa)(\Lambda/H)^{(\kappa-1)/\kappa}$ (7). In practice, this factor becomes important mainly when Ω is large, i.e., when Φ goes

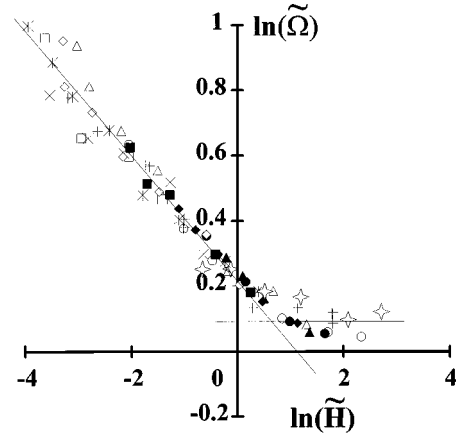


FIG. 5. Variations of $\ln \tilde{\Omega} = \ln[\Omega/(\Gamma/D)^{1/(\kappa-1)}]$ as a function of $\ln \tilde{H} = \ln[H/\Lambda(D/\Gamma)^{\kappa/(\kappa-1)}]$. The symbols are the same as in Figs. 2 and 3. The solid lines correspond to the scaling laws predicted in domains I and II [Eqs. (5) and (6)].

to Φ^{**} . Finally, we can calculate the equation of the line that separates domains I and II in Fig. 4. The crossover that corresponds to $D/H=4\mu\alpha\Omega$ is expressed as $D/\Gamma \sim (H/\Lambda)^{(\kappa-1)/\kappa}$ (8).

Let us now return to the experiments. In a broad range of volume fractions, the variation of Ω versus Φ follows a power law as expected from Eq. (6) (see Fig. 1). When Ω goes to 1, the discrepancy observed with the scaling law is well described by the correcting factor introduced previously (7). In the same way, the variations of Ω versus H measured for various values of Φ also follow power laws in a broad range of H (see Fig. 2). All these points belong to domain II in Fig. 4. The exponents and the prefactors found by fitting these different sets of data lead to same values for κ and σ_0 : $\kappa=5.5 \pm 0.5$ and $\sigma_0=5 \times 10^{10}$ N/m². It is worth noting that in this regime, Ω is also expected to be independent of D ; this agrees well with what is observed for large values of D (see Fig. 3). Let us now consider the crossover between domains II and I. In Fig. 2, for Φ larger than 3×10^{-3} , Ω goes to a constant value as H increases. This observation agrees well with expression (5), which predicts that, in domain I Ω is independent of H . Furthermore, as Φ increases, the crossover between the two types of behavior takes place for decreasing values of H , as expected from expression (8). In the same way, in Fig. 3, Ω is observed to increase as D decreases, the crossover taking place for larger values of D as Φ increases. Figure 5 is a log-log representation of the variations of $\Omega/(\Gamma/D)^{1/(\kappa-1)}$ as a function of $H/\Lambda(D/\Gamma)^{\kappa/(\kappa-1)}$. Using this set of coordinates, the points measured for different values of Φ , H , and D all fall on a universal curve, as expected.

In summary, our simplified model of sediment equilibrium allows a good interpretation of systematic measurements of sediment relative volume. Contrary to usual situations where sediments are incompressible, we show that the sediments formed by aggregated colloidal suspension compact under their own weight following remarkable scaling behaviors. As a consequence, the volume fraction Φ^{**} that separates the regime where the suspension is stable under

gravity from the regime where the suspension separates is not intrinsic to the physicochemical system but depends on the height and width of the sample and on the friction between the gel and the vertical wall side.

We are grateful to J. F. Argillier, J. Hinch, and J. Lecourtier for enlightening discussions. Laboratoire “Fluides, Automatique et Systèmes Thermiques” is a laboratory of Paris VI and is associated with CNRS (URA 871) and Paris XI.

-
- [1] *Kinetics of Aggregation and Gelation*, edited by F. Family and D. P. Landau (North-Holland, Amsterdam, 1984).
- [2] R. Jullien, *Croatia Chem. Acta* **65**, 215 (1992).
- [3] M. L. Broide and R. J. Cohen, *Phys. Rev. Lett.* **64**, 2026 (1990).
- [4] M. Carpineti, F. Ferri, M. Giglio, E. Paganini, and U. Perini, *Phys. Rev. A* **42**, 7347 (1990).
- [5] S. Stoll and E. Pefferkorn, *J. Colloid Interface Sci.* **152**, 247 (1992).
- [6] M. Couch, Ph.D. thesis, Cambridge University, 1993 (unpublished).
- [7] M. Wafra, Ph.D. thesis, Université Paris XIII, 1994 (unpublished).
- [8] C. Allain, M. Cloitre, and M. Wafra, *Phys. Rev. Lett.* **74**, 1478 (1995).
- [9] C. Allain, M. Cloitre, and F. Parisse, *J. Colloid Interface Sci.* **178**, 411 (1996).
- [10] D. Senis and C. Allain, *J. Inst. Fr. Pet. (France)* (to be published).
- [11] N. J. Alderman, G. H. Meeten, and J. D. Sherwood, *J. Non-Newtonian Fluids Mech.* **39**, 291 (1991).
- [12] R. Buscall, P. D. A. Mills, J. W. Goodwin, and D. W. Larson, *J. Chem. Soc. Faraday Trans. 1* **84**, 4249 (1988).
- [13] K. A. Landman and W. B. Russel, *Phys. Fluids A* **5**, 550 (1993).